

Photoacoustic properties of softmagnetic amorphous $\text{Fe}_{81}\text{B}_{13}\text{Si}_4\text{C}_2$ ribbon

D. VASILJEVIĆ-RADOVIĆ, P. M. NIKOLIĆ, D. M. TODOROVIĆ, O. S. ALEKSIĆ
Joint Laboratory for Advanced Materials of SASA, P.O. Box 745, 11000 Beograd, Yugoslavia

J. ELAZAR, Z. RISTOVSKI, V. BLAGOJEVIĆ
Faculty of Electrical Engineering, Belgrade University, P.O. Box 816, Belgrade, Yugoslavia

Photoacoustic properties of amorphous $\text{Fe}_{81}\text{B}_{13}\text{Si}_4\text{C}_2$ ribbons were investigated. The amplitude and phase photoacoustic spectra were measured as a function of the modulation frequency of an He–Ne laser beam. Thermal diffusivity was determined by comparison of obtained experimental results and calculated theoretical photoacoustic spectra for a non-annealed $\text{Fe}_{81}\text{B}_{13}\text{Si}_4\text{C}_2$ sample and an $\text{Fe}_{81}\text{B}_{13}\text{Si}_4\text{C}_2$ sample annealed at 600 °C.

© 1998 Chapman & Hall

1. Introduction

Since Rosenzweig [1] revived photoacoustic (PA) spectroscopy, in the early eighties, various photothermal methods have been used to detect temperature changes due to irradiation of a sample with a periodically modulated light beam [2–4]. The PA method is widely used for the investigation of thermal, optical and even transport properties of materials. The PA effect represents a process of the generation of acoustical waves in a material after the absorption of a modulated energy beam. After this absorption many thermal and the other deexcitation processes can appear.

The PA signal can be detected using various configurations. In this work the excitation of the sample was on one side, while detection of the acoustic response was on the other side, e.g. the so called heat transmission configuration was used. The heat that transferred through the sample can be defined by thermal diffusivity, D_T , which is defined as the ratio between thermal conductivity, K , heat capacity, C_T , and density, ρ .

In this paper thermal diffusivity of an amorphous $\text{Fe}_{81}\text{B}_{13}\text{Si}_4\text{C}_2$ commercial ribbon is investigated. A modified open PA cell (MOPC) detection technique was used, which has a much better signal–noise ratio compared with the construction previously explained in the literature [5–7].

2. Experimental procedure

The experimental amplitude and phase PA spectra were obtained using a specially constructed PA cell [8], which was an MOPC. Its construction was optimized to obtain maximal acoustical protection from surrounding influence. In that way a very good signal–noise ratio and a flat frequency characteristic in the frequency range 60–600 Hz were obtained. The modification made possible the obtaining of high quality PA amplitude and phase signals compared with similar previously published experimental

diagrams [9, 10]. In Fig. 1 the geometry of the PA cell used in this investigation is given.

Amorphous $\text{Fe}_{81}\text{B}_{13}\text{Si}_4\text{C}_2$ ribbons were measured using an He–Ne laser as an optical source. The laser beam was modulated by an acousto-optical modulator and the sample was irradiated by a large spot (about 6 mm in diameter) in order to eliminate the effect of lateral diffusion in the measured sample. A sample holder of the PA cell was used which required a disc shaped sample with a maximum diameter of 9.5 mm. Each sample was mounted directly onto the front side of an electret microphone, which had a circular window of 3 mm diameter as the sound inlet. The $\text{Fe}_{81}\text{B}_{13}\text{Si}_4\text{C}_2$ ribbon was 30 μm thick.

In Fig. 2a, b PA signal amplitude and phase diagrams, versus the modulation frequency, for a non-annealed commercial $\text{Fe}_{81}\text{B}_{13}\text{Si}_4\text{C}_2$ sample are given, respectively. Experimental values are shown by dots, while the fitted theoretical curve is given by a full line.

In Fig. 3a, b the amplitude and phase spectra versus modulation frequency, for the same sample but annealed at 600 °C, are given, respectively.

3. Discussion

Theoretical explanation and analysis of the experimental results is based on the thermal piston model of Rosenzweig and Gersho [2] where the PA signal is due to the periodic temperature variations on the boundary sample–gas surface which can be calculated using the equation

$$\delta P = \gamma \frac{P_0 \theta_s}{T_0 l_g \sigma_g} \exp(j\omega t) \quad (1)$$

where P_0 and T_0 are the ambient pressure and temperature; l_g is the thickness of the gas; $\sigma_g = (1 + j)a_g$; $a_g = (\pi f / D_{gT})^{1/2}$, where a_g is the thermal diffusion coefficient in gas, with thermal diffusivity, D_{gT} , and γ is the adiabatic constant of the gas. The samples'

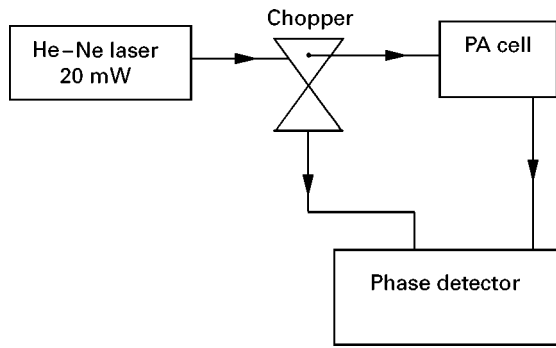


Figure 1 The experimental setup of a modified open photoacoustic cell with a heat transmission configuration.

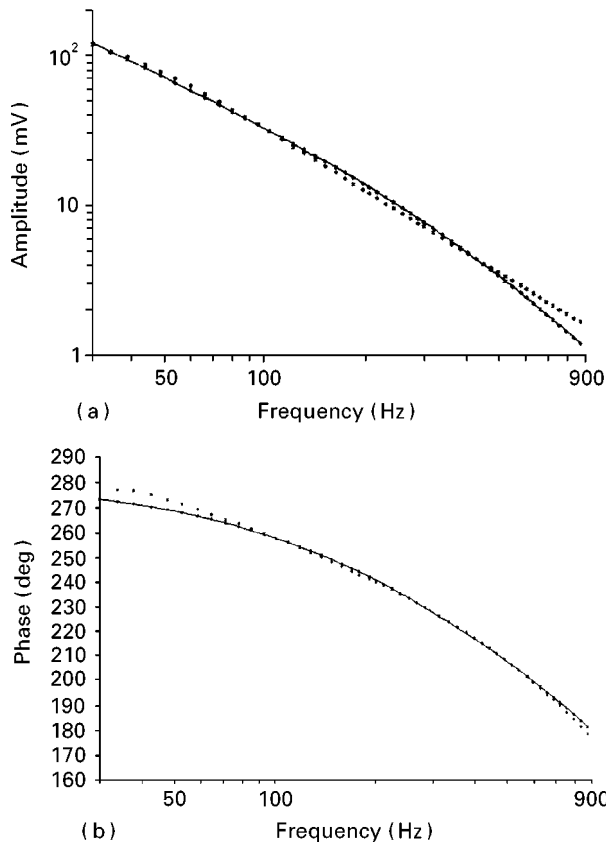


Figure 2 Theoretical (—) and experimental (···) amplitude (a) and phase diagrams (b), versus modulation frequency for a non-annealed $\text{Fe}_{81}\text{B}_{13}\text{Si}_4\text{C}_2$ sample.

temperature fluctuation, at the sample backing interface, θ_s , is an essential feature which should be obtained. There are several one-dimensional theoretical approximate [9] modes which can be used to determine thermal properties of $\text{Fe}_{81}\text{B}_{13}\text{Si}_4\text{C}_2$ samples.

The distribution of the periodic part of the thermal flux, θ , is determined by solving the following system of differential equations

$$\left(\frac{d^2}{dx^2} - \sigma_i^2\right)\theta_i = \begin{cases} 0 & i = \text{g, b} \\ -\frac{\alpha I_0}{2k_s} \exp^{-\alpha x} & i = \text{S} \end{cases} \quad (2)$$

where $\sigma_i^2 = j\varepsilon/D_{Ti}$; D_{Ti} is thermal diffusivity of the layer i ; s, g and b denote "sample", "gas" and "backing", respectively.

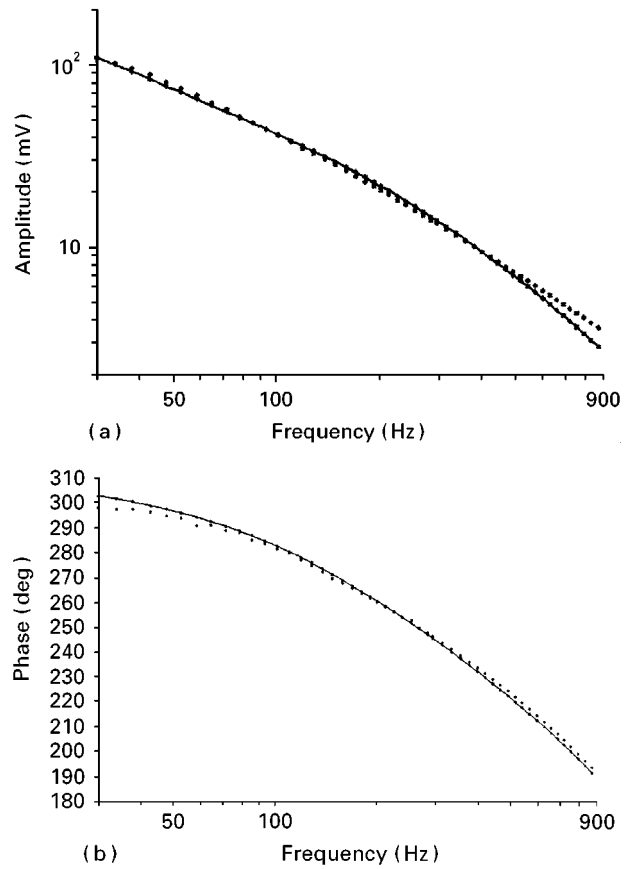


Figure 3 Theoretical (—) and experimental (···) amplitude (a) and phase spectra (b), versus modulation frequency for an $\text{Fe}_{81}\text{B}_{13}\text{Si}_4\text{C}_2$ annealed sample at 600°C .

According to the Rosenzweig and Gersho theory [2] the solution of Equation 2 for the case of a heat transmission configuration is

$$\theta_s = \frac{2I_0}{k_s \sigma_s \sinh(\sigma_s l)} \quad (3)$$

where k_s is the thermal conductivity, I_0 is the intensity of the incident light and l is the thickness of the sample.

The experimental amplitude and phase PA signals were corrected in the modulation frequency range 10–100 Hz. Analysis of the experimental amplitude and phase PA signals, versus modulation frequencies, have shown that for frequencies below 60 Hz, the PA signals decrease. The reason for this is a decrease in the microphone sensitivity. To correct this, the following procedure was performed.

First, the amplitude PA signal, for a reference sample, was measured. This was a thin Al tape (25 μm thick). For this reference sample the theoretical amplitude PA signal was calculated (using Equations 1 and 3) and then fitted with the experimental one. Agreement between the experimental data for the reference sample and the theoretical predictions was very good except in the frequency range < 100 Hz. The difference between these experimental and theoretical fitted curves were then used as an amplitude correction factor. Therefore, all the experimental amplitude PA signals of $\text{Fe}_{81}\text{B}_{13}\text{Si}_4\text{C}_2$ samples were multiplied with the previously obtained amplitude correction factors.

Second, the corrected experimental amplitude PA signals for $\text{Fe}_{81}\text{B}_{13}\text{Si}_4\text{C}_2$ samples were fitted in the frequency range 10–100 Hz with the theoretical calculated PA signals. In this case only thermal diffusivity was used as a fitting parameter. Using this procedure of amplitude fitting the phase PA diagram for the same $\text{Fe}_{81}\text{B}_{13}\text{Si}_4\text{C}_2$ sample was calculated. The difference between the experimental and theoretical phase diagrams was then used to calculate the phase correction factors versus frequency, which were then used to correct the experimental phase of all remaining $\text{Fe}_{81}\text{B}_{13}\text{Si}_4\text{C}_2$ samples. These phase corrections were necessary only for frequencies < 100 Hz.

The experimental amplitude phase PA spectra were compared with theoretical calculated diagrams. The values of thermal diffusivity and absorption coefficient for commercial non-annealed $\text{Fe}_{81}\text{B}_{13}\text{Si}_4\text{C}_2$ and annealed (at 600°C) samples, are given in Table I.

These data cannot be compared with any literature values, because as far as is known they do not exist, so it is interesting to compare them with the properties of pure Fe and B. For instance thermal diffusivity for Fe is about $0.2 \times 10^{-4} \text{ m}^2 \text{ s}^{-1}$ and for boron, $D_T = 0.5 \times 10^{-6} \text{ m}^2 \text{ s}^{-1}$. The value for the annealed $\text{Fe}_{81}\text{B}_{13}\text{Si}_4\text{C}_2$ sample was the same as for pure boron. The thermal diffusivity for the non-annealed $\text{Fe}_{81}\text{B}_{13}\text{Si}_4\text{C}_2$ sample was about 50% higher.

This difference can be explained by the change of structure of the measured sample. The absorption coefficient of the annealed sample was slightly bigger compared to the non-annealed sample. It is difficult to say that this difference in the absorption coefficient

was the consequence of the change of the crystal structure. Its surface was more rough after annealing and this may be the reason for this difference.

4. Conclusions

In this work the authors have carried out, for the first time, an investigation of thermal diffusivity of amorphous $\text{Fe}_{81}\text{B}_{13}\text{Si}_4\text{C}_2$ ribbons using a photoacoustic method with a heat-transmission configuration.

The thermal diffusivity for a non-annealed commercial $\text{Fe}_{81}\text{B}_{13}\text{Si}_4\text{C}_2$ sample was $D_T = 0.73 \times 10^{-6} \text{ m}^2 \text{ s}^{-1}$, which decreased to $0.5 \times 10^{-6} \text{ m}^2 \text{ s}^{-1}$ when the sample was annealed at 600°C . It was demonstrated that the heat transmission PA method, as a contactless method can be successfully used for the determination of thermal diffusivity.

References

1. A. ROSENCWAIG, *Opt. Commun.* **7** (1973) 305.
2. A. ROSENCWAIG and GERSHO, *J. Appl. Phys.* **47** (1976) 64.
3. A. MANDELIS, "Photoacoustic and Thermal Wave Phenomena in Semiconductors" (North-Holland, New York, 1987).
4. H. VARGAS and L. C. M. MIRANDA, *Phys. Rev. B* **161** (1988) 43.
5. L. F. PERONDI and L. C. M. MIRANDA, *J. Appl. Phys.* **62** (1987) 2955.
6. D. M. TODOROVIĆ, P. M. NIKOLIĆ, D. G. VASILJEVIĆ and M. D. DRAMIĆANIN, *ibid.* **78** (1994) 4012.
7. M. D. DRAMIĆANIN, P. M. NIKOLIĆ, Z. D. RISTOVSKI, D. G. VASILJEVIĆ and D. M. TODOROVIĆ, *Phys. Rev. B.* to be published.
8. D. M. TODOROVIĆ and P. M. NIKOLIĆ, Report to Physical Chemistry of Materials, 15–16 November 1994, Belgrade, p. 18.
9. A. PINTO NETO, H. VARGAS, N. LEITE and L. C. M. MIRANDA, *Phys. Rev. B* **40** (1989) 3924.
10. *Idem, ibid.* **41** (1990) 3924.

TABLE I The values of thermal diffusivity and absorption coefficient for $\text{Fe}_{81}\text{B}_{13}\text{Si}_4\text{C}_2$ samples

	$D_T(\text{m}^2 \text{ s}^{-1})$	$\alpha(\text{cm}^{-1})$
$\text{Fe}_{81}\text{B}_{13}\text{Si}_4\text{C}_2$ Non-annealed	0.73×10^{-6}	4.9×10^{11}
Annealed at 600°C	0.50×10^{-6}	1.3×10^{12}

Received 22 February
and accepted 17 July 1996